



Potential of a probabilistic hydrometeorological forecasting approach for the 28 September 2012 extreme flash flood in Murcia, Spain



A. Amengual ^{*}, V. Homar, O. Jaume

Grup de Meteorologia, Departament de Física, Universitat de les Illes Balears, Palma, Mallorca, Spain

ARTICLE INFO

Article history:

Received 10 March 2015

Received in revised form 11 June 2015

Accepted 12 June 2015

Available online 19 June 2015

Keywords:

Flash-flood

Mesoscale convective system

Hydrological modeling

Ensemble prediction system

ABSTRACT

An improved understanding, modeling and forecasting of hydrometeorological extremes over the flood-prone Western Mediterranean region is one of the milestones of the international HyMeX program. A set of severe hydrometeorological episodes affected various basins across south and eastern Mediterranean Spain from 27 to 29 September 2012. Flooding was particularly catastrophic in Andalusia and Murcia, where 10 fatalities occurred and material losses were estimated at 120 M€. The predictability bounds set by the type and scales of the processes involved in such high-impact episodes require the explicit representation of uncertainty in the hydrometeorological forecasting chain. A short-range ensemble prediction system (EPS) provides the optimal framework to generate risk-based forecasts supporting valuable early warning procedures and mitigation measures. We explore the potential of this probabilistic forecasting approach on the 28 September 2012 flash flood in the Guadalentín river basin, a medium-sized catchment located in Murcia, southeastern Spain. After a rigorous calibration with rain-gauge data, the hydrological response of the basin to this flooding is accurately simulated by the Hydrologic Engineering Center's Hydrological Modeling System runoff model. Then, we explore the uncertainty transference from a collection of mesoscale meteorological deterministic and probabilistic 48 h predictions provided by the Weather Research and Forecasting (WRF) model. The meteorological simulations are nested within the global EPS of the European Centre for Medium-Range Weather Forecasts, therefore inheriting the spread of the global system and providing probabilistic high-resolution precipitation structures to the hydrological model. By assuming the calibrated model as a good representation of a perfect hydrological model for this event, it becomes an advanced and user-oriented verification tool for quantitative precipitation forecasts. Results highlight the benefits of accounting for uncertainties in the precipitation forecasts and the value of the proposed set-up for the short-range prediction of quantitative discharge forecasts. The warn-on-forecast approach is shown to be possible within a probabilistic hydrometeorological forecasting chain for basins as small and fast-responsive as the Guadalentín basin, proving to be suitable for civil protection warning procedures.

© 2015 Elsevier B.V. All rights reserved.

1. Introduction

The HyMeX (HYdrological cycle in the Mediterranean EXperiment, <http://www.hymex.org>) program is an international effort aimed at advancing in the scientific knowledge of the water cycle variability from a seamless approach. One of the major scientific challenges of HyMeX is to improve the understanding of hydrometeorological extremes in the Western Mediterranean (Drobinski et al., 2014). Heavy precipitation and flash flooding are among the most devastating natural hazards in terms of loss of human life and property. Flash floods are a consequence of high precipitation rates persisting for several hours over a specific basin. This persistence is often associated with prominent orography that anchors quasi-stationary mesoscale convective systems (MCSs; Doswell et al., 1996; Kolios and Feidas, 2010).

The Western Mediterranean is prone to heavy precipitation and flash flooding during late summer and early autumn (Llasat et al., 2010). The sensible and latent heat fluxes from the relatively high sea surface temperature of the Mediterranean Sea increase the convective available potential energy (CAPE) of the overlying air masses. Together with the intrusion of high lapse rates in the lower mid-troposphere, the complex orography and land–sea contrasts promote the lifting of low-level conditionally unstable air, favoring the triggering of moist convection. The accurate understanding and prediction of all these factors are critical when seeking to mitigate the impacts of heavy rainfalls, which combined with densely urbanized coastal areas and specific geographical settings of this region (Fig. 1), often result in hazardous and sudden flash floods (Drobinski et al., 2014; Ducrocq et al., 2014).

Indeed, small and medium size coastal steep basins and high urbanization rates imply short hydrological response times. These short time scales reduce the effectiveness of warning systems driven by rainfall observations for implementing precautionary civil protection measures

^{*} Corresponding author at: Arnau Amengual, Dept. de Física, Universitat de les Illes Balears, 07122 Palma, Mallorca, Spain.

E-mail address: arnau.amengual@uib.es (A. Amengual).

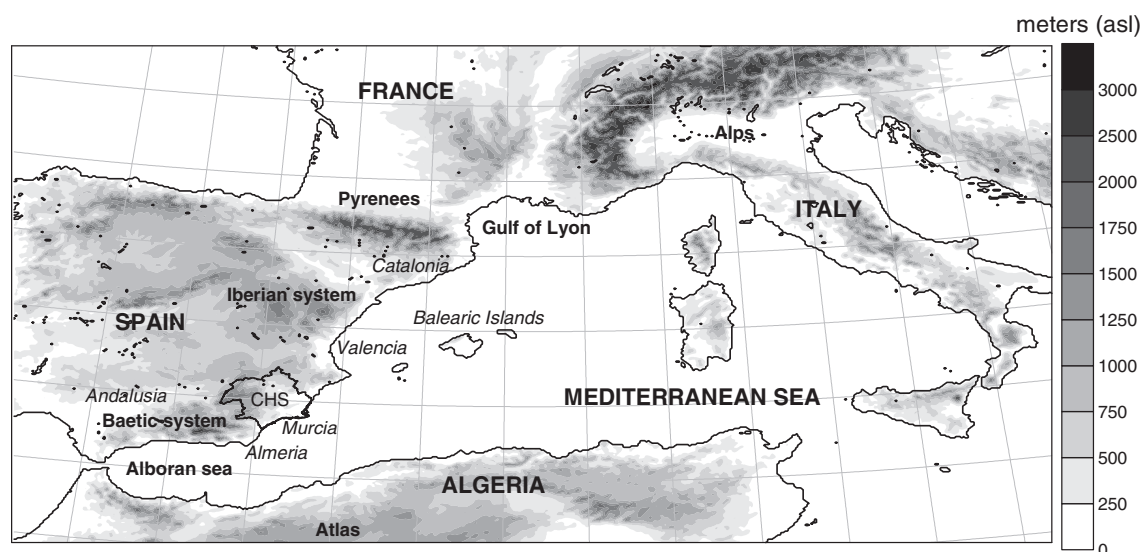


Fig. 1. Configuration of the computational domain used for the WRF numerical simulations. Main geographical features mentioned in the text are shown. The thick continuous line shows the CHS region where the Guadalentín river basin is located.

(Siccardi, 1996). Nowadays, short-range quantitative precipitation forecasts (QPFs) from convection-permitting meteorological models can be effectively used to drive hydrological systems, thus extending the civil warning lead-times. However, to predict within tolerable precisions the location and timing of high precipitation rates, as well as rainfall amounts are particularly challenging for the current deterministic operational configurations. Relatively small errors in the QPF fields can even lead to misleading quantitative discharge forecasts (QDFs) for medium- and small-sized basins, that prevent any early flood warning procedure from being accurate and dependable. It is well known that the hydrometeorological forecasting chain is affected by several sources of error that should be accounted for when designing any operational system (Bartholmes et al., 2009; Cloke et al., 2013). These errors arise from the hydrological and meteorological model formulations, their initial and boundary conditions and from the scale-gap between both systems (Zappa et al., 2011). To cope with these problematics, flood forecasting is increasingly dependent on high-resolution ensemble prediction systems (EPSs; Cloke and Pappenberger, 2009). When using an EPS to drive a hydrological model, a hydrological ensemble prediction system (HEPS) is generated. In recent years, considerable efforts are being made to demonstrate and quantify the added value provided by HEPSs (Verbunt et al., 2007; Amengual et al., 2008, 2009; Vincendon et al., 2011; Cloke et al., 2013).

Within this framework, we examine the intense precipitations that occurred from 27 to 29 September 2012 over wide areas of southern and eastern Mediterranean Spain. The resulting flash floods caused 10 fatalities in Andalusia and Murcia, and 120 M€ of estimated material losses. To investigate the predictability of such extremes in medium-sized catchments, we focus on the 28 September flash flood over the Guadalentín river basin located in Murcia, southeastern Spain (Figs. 1 and 2). We assess the potential of an EPS strategy versus a deterministic approach in order to provide a useful basis for flood early warning procedures and mitigation measures. First, we analyze the available rain-gauge observations and calibrate the hydrologic runoff model. Next, we generate an ensemble of high-resolution mesoscale predictions with 48 h as lead time by downscaling the global European Centre for Medium-Range Weather Forecasts Integrated Forecast System (ECMWF IFS) ensemble forecasts. Perturbations in the global system are derived from flow-dependent singular vectors (Buizza and Palmer, 1995; Molteni et al., 1996) computed daily at ECMWF to span the synoptic-scale uncertainties of the day.

Finally, the verification of QPFs is not performed using classical pointwise measures as hydrological purposes rely on integrated values of precipitation over the watershed surface. From a certain perspective, we use the hydrological model as an advanced NWP validation tool, and particularly to verify the QPF field for a primary end-user such as a hydrological warning system. Admitting that no perfect forecast can be rendered with the currently available prediction systems, mesoscale model evaluation exercises based on relevant QPF applications, such as the analysis of its hydrological response, are meaningful (Benoit et al., 2003; Jasper and Kaufmann, 2003; Chancibault et al., 2006; Amengual et al., 2008, 2009). The rest of the paper is structured as follows: Section 2 consists of a brief description of the study area and the rain- and flow-gauge networks; Section 3 describes the hydrometeorological episode; Section 4 presents the hydrological tools used for the basin characterization and to set-up the driven runoff experiments; Section 5 describes the meteorological tools; Section 6 presents the experiments and discusses the results. Section 7 provides an assessment of the methods used, including further remarks.

2. The study area

2.1. Overview of the Guadalentín river basin

The Guadalentín river is the most important tributary of the Segura river basin. The Segura is the third largest Spanish river flowing into the Mediterranean, with an extension of 18,208 km² and a length of about 325 km (Fig. 1). The Guadalentín river basin extends from the Baetic system – with heights above 2000 m, through the Murcia pre-litoral depression – with elevations up to 1200 m – and its river valley, which ends at the junction with the Segura and has heights about 110 m. The Guadalentín has a whole drainage area of 3343.1 km² and a maximum length close to 121 km (Fig. 2). The river is located in one of the most arid regions of Spain. The Baetic System shelters this region from the passage of the rainfall-bearing Atlantic cold fronts. Thus, precipitation mainly comes from south-easterly moist flows associated with subsynoptic-scale, less frequent Mediterranean disturbances. Annual precipitations range from above 500 mm to barely 300 mm, depending on altitude. The rainfall regime is typical of the Spanish Mediterranean area, with most heavy rainfall episodes occurring in late summer and early autumn. These extreme rainfall events can account for a very large fraction of the annual amounts.

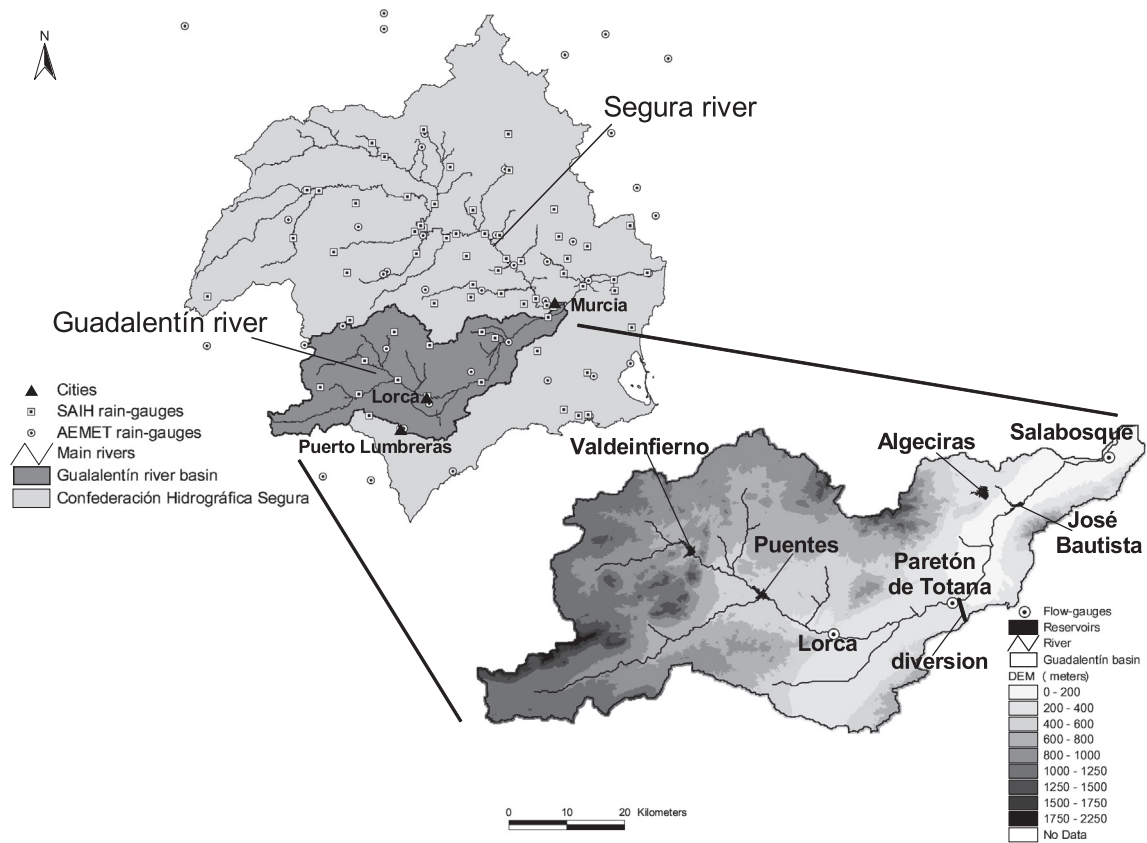


Fig. 2. Distribution of the rain-gauges from the Automatic Hydrological Information System (SAIH; 66 stations) of the CHS and the Agencia Estatal de Meteorología (AEMET; 42 stations). It includes a total of 108 automatic rainfall stations distributed over an area of 18,208 km². The Guadalentín river basin is highlighted in shaded dark gray. Digital terrain model of the Guadalentín river basin with a cell size of 100 m is also shown. Main tributaries, stream-gauges, reservoirs and the artificial channel connecting the river, just downstream of Paretón de Totana, and the Mediterranean Sea are indicated.

Owing to this semi-arid environment, the Guadalentín river is characterized by a very irregular regime, passing from large periods of very low flows – annual mean discharge is scarcely $1.35 \text{ m}^3 \text{ s}^{-1}$ – to sporadic flash floods of great magnitude (Gil-Olcina, 1968). Being aware of the recurrent nature of these episodes, many elements of flood control and water supply have been introduced within the internal catchments of the Segura. In particular, four reservoirs are located along the Guadalentín river and an artificial channel connects the river, just downstream of Paretón de Totana, and the Mediterranean Sea (Fig. 2). Thus, large discharge and sediment volumes are partially diverted into the Mediterranean in order to avoid catastrophic flooding in Murcia city. Despite these infrastructures, extreme episodes still pose significant threats to life and property. For instance, two extreme flash-floods resulted in high-societal impacts within the Guadalentín basin. On 19 October 1973, 89 people were killed in Puerto Lumbreras and 13 additional fatalities occurred in Lorca; and on 2 September 1989, a flash flood produced 3 casualties and serious material damage (Capel, 1974, 1989).

2.2. The rain and stream gauge networks

The raw precipitation data available to study the case comes from 108 stations providing 5-min accumulations within or close to the Confederación Hidrológica del Segura (CHS) demarcation (Fig. 2). These pluviometric stations are distributed over an area of 18,870 km² and belong either to the Automatic Hydrological Information System (SAIH) network of the CHS or to Spanish Agency of Meteorology (AEMET). Nearly 40 of these stations lie within the Guadalentín basin or near its boundaries. Runoff data at 5-min intervals is also available at three flow gauges along the basin, which are integrated in the SAIH

network. These stream-gauges are located in Lorca and Paretón de Totana cities and in Salabosque – a suburb of Murcia city, with drainage areas of 1827.1 km², 2384.7 km² and 3170.4 km², respectively (Fig. 2).

3. Description of the 28 September 2012 hydrometeorological episode

The synoptic evolution during the hours preceding the active unfolding of the convective episode was mainly characterized by a remarkable Potential Vorticity (PV) streamer forming from north-western Europe towards the Madeira Island area on 26 September. During the early hours of 27 September, this PV streamer moved eastward while narrowing and eventually breaking from the main westerlies and forming a closed low southwest of the Iberian Peninsula on 27 September 12 UTC (Fig. 3). This strong closed system moved slowly eastward along the southern and eastern Iberian Peninsula from 27 through 29 September. Several authors have identified the forward flank region of such PV streamers as favorable for the development of deep convection (Doswell et al., 1998; Schumann and Roebber, 2010). These upper-level anomalies contribute not only to the dynamical uplift by PV advection, but also to the convective destabilization by the intrusion of cold air aloft associated with high lapse rates within the trough.

At low levels, cold air advanced over the western North Atlantic along with the upper-level PV streamer on 26 September. Cyclogenesis occurred over the southwestern Iberian Peninsula as the upper-level PV anomaly was splitting from the main PV reservoir associated with the general westerlies (Fig. 4). The circulation associated to the cyclone contributed to the strengthening of the cold front over the Moroccan Atlantic coast and, as it intensified, warm African air was brought to the north, generating a warm front on its eastern–northeastern forward

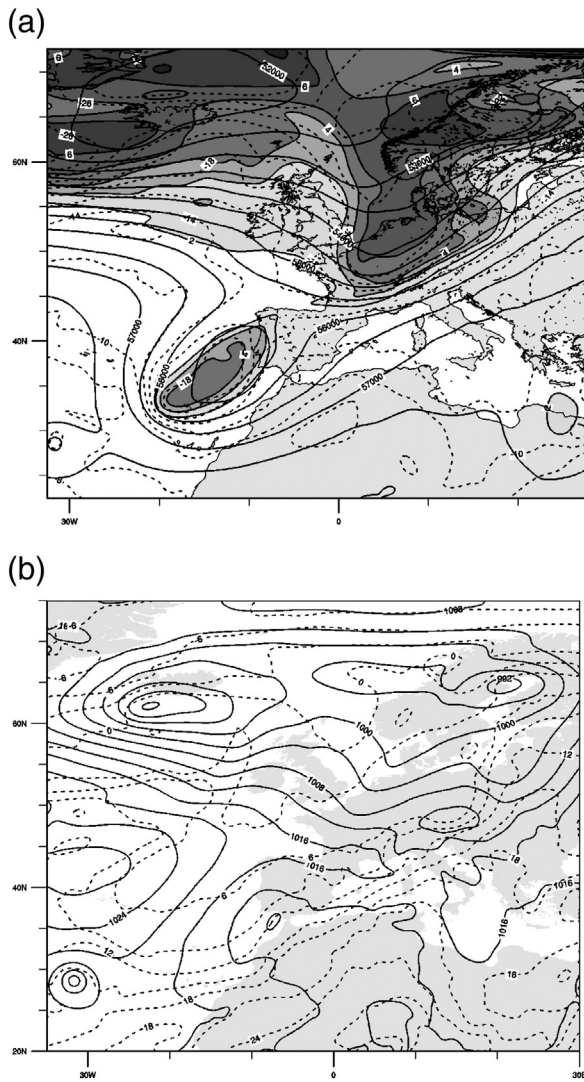


Fig. 3. ECMWF analysis at 12 UTC on 27 September 2012: (a) geopotential (solid lines, in gpm), temperature (dashed, in °C) at 500 hPa and potential vorticity (PVU, shaded), (b) mean sea level pressure (solid lines, hPa) and temperature at 850 hPa (dashed, in °C).

flank. The evolution of this classical baroclinic structure at low levels was the key not only to destabilize the low-level parcels, but also to set up the appropriate mesoscale flows to feed the convective systems with warm and moist unstable air transported over the relatively warm Mediterranean Sea surface.

Similar to the mechanism observed in other western Mediterranean episodes, important rainfall occurred in the overlapping area of the upper-level anomaly and the lower-levels warm and moist easterly advection. Convection organized in bands and frequently anchored by the complex orography of the region produced extraordinary torrential precipitations over Almería and Murcia. The main convective systems were associated with a convergence zone between the warm and moist easterly advection produced by the low-level cyclone and the remnants of the synoptic-scale cold Atlantic intrusion. This convergence zone, together with the aforementioned strong dynamical indicators of ascent on the northeasterly flank of the upper-level trough and the complex orography of the region, resulted in the generation of a quasi-stationary and V-shaped MCS that lasted several hours over Murcia (Ducrocq et al., 2014). Daily precipitation amounts reached 214 mm in parts of Andalusia and 240 mm in Murcia (Fig. 5a).

Over the Guadalentín river basin, most of the torrential precipitation occurred between 06 and 14 UTC on 28 September. Accumulated 5-min and 1-h quantities were above 37 and 119 mm in some locations. An

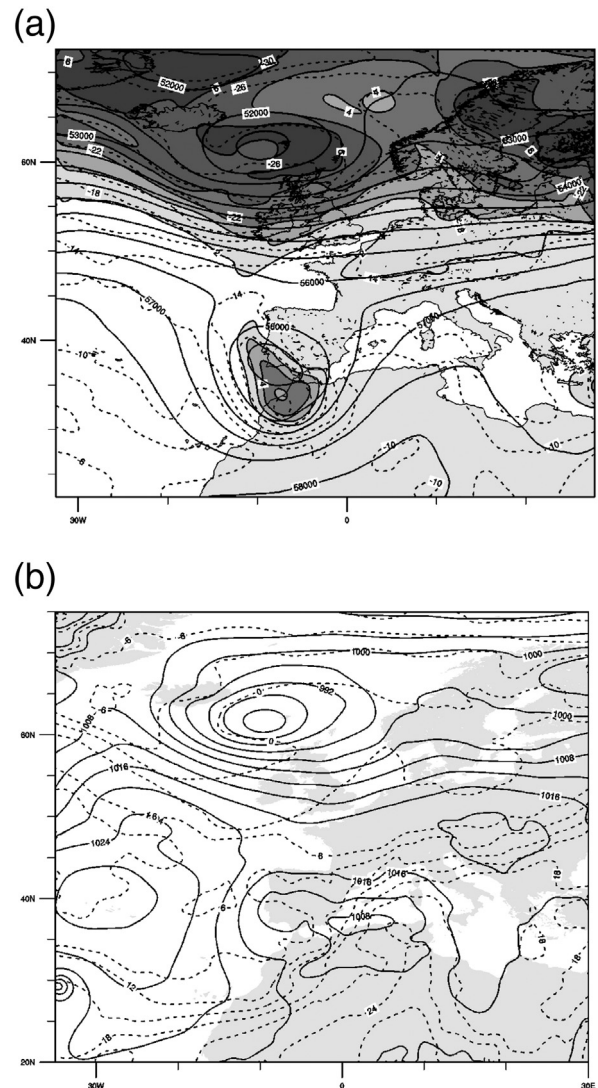


Fig. 4. As in Fig. 3, but for 12 UTC on 28 September 2012.

accumulated maximum of 214 mm in 8 h was recorded in the southernmost part of the catchment (Fig. 6a). The maximum discharge at Lorca was of $616.3 \text{ m}^3 \text{ s}^{-1}$ at 13:15 UTC (Fig. 7a). In Paretón de Totana, barely 20 km downstream of Lorca, two almost consecutive peak discharges of 1067.9 and $1081.2 \text{ m}^3 \text{ s}^{-1}$ were observed at 16 UTC and 17:20 UTC, respectively (Fig. 7b). Peak flows up to $939.7 \text{ m}^3 \text{ s}^{-1}$ were diverted into the Mediterranean Sea by the artificial channel that connects the Guadalentín river with the Mediterranean Sea. Thus, peak discharges were significantly reduced – and later abated by the José Bautista reservoir – to two maximums of 55.2 and $54.5 \text{ m}^3 \text{ s}^{-1}$ at 16 and 19 UTC, respectively, in Salabosque (Fig. 7c). This flash-flooding produced 4 fatalities, the evacuation of many inhabitants in Puerto Lumbreras and Lorca, and material losses exceeded 64 M as several infrastructures were destroyed.

4. Hydrological tools

4.1. Rainfall–runoff model description

We simulate the hydrological response of the Guadalentín basin by using the HEC-HMS rainfall–runoff model (USACE-HEC, 1998). The model has been implemented in a semi-distributed and event-based configuration. The Guadalentín basin has been segmented into 27 sub-basins with an average size of 117.4 km^2 and a total extension of

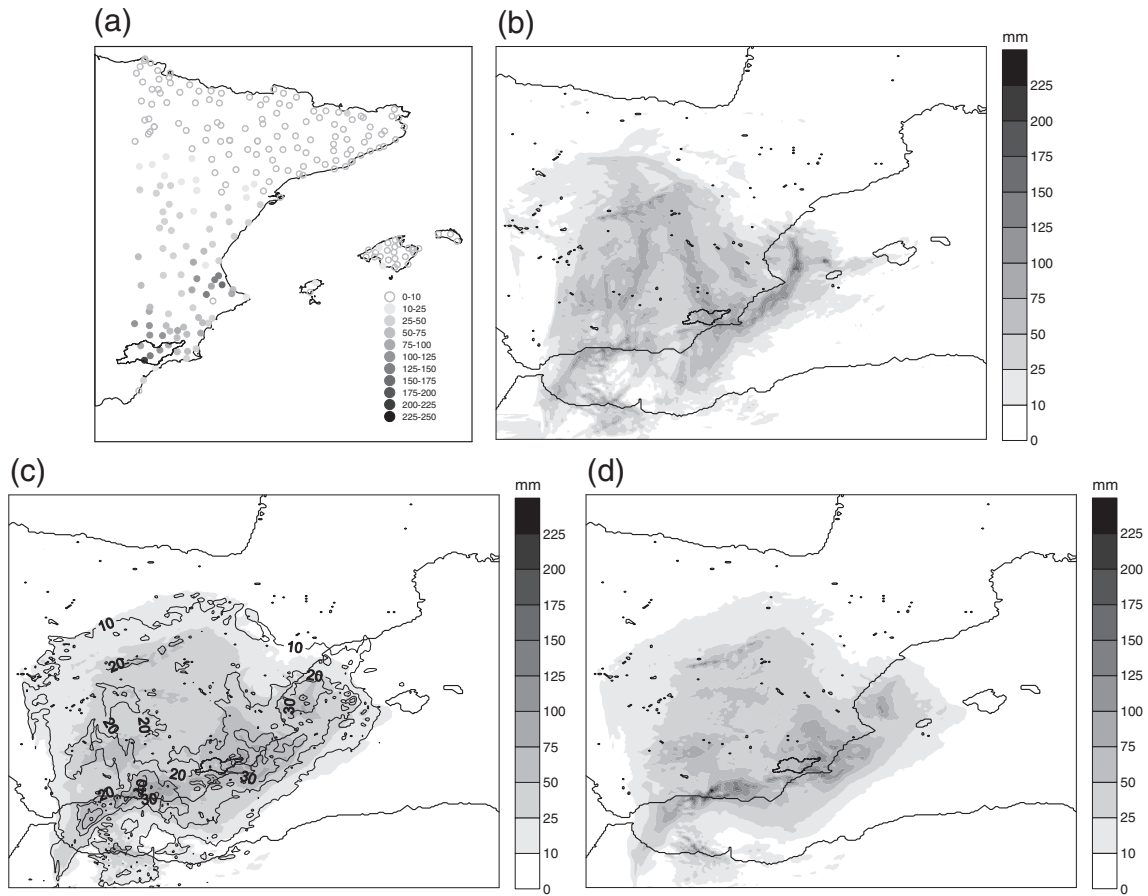


Fig. 5. Observed (a), control (b), ensemble mean and standard deviation (c), and probability-matched ensemble mean (d) accumulated precipitation fields from 27 to 29 September 2012 at 00 UTC. Shaded contours according to the scale. Standard deviations also shown as black lines, in mm. The Guadalentín river basin is highlighted.

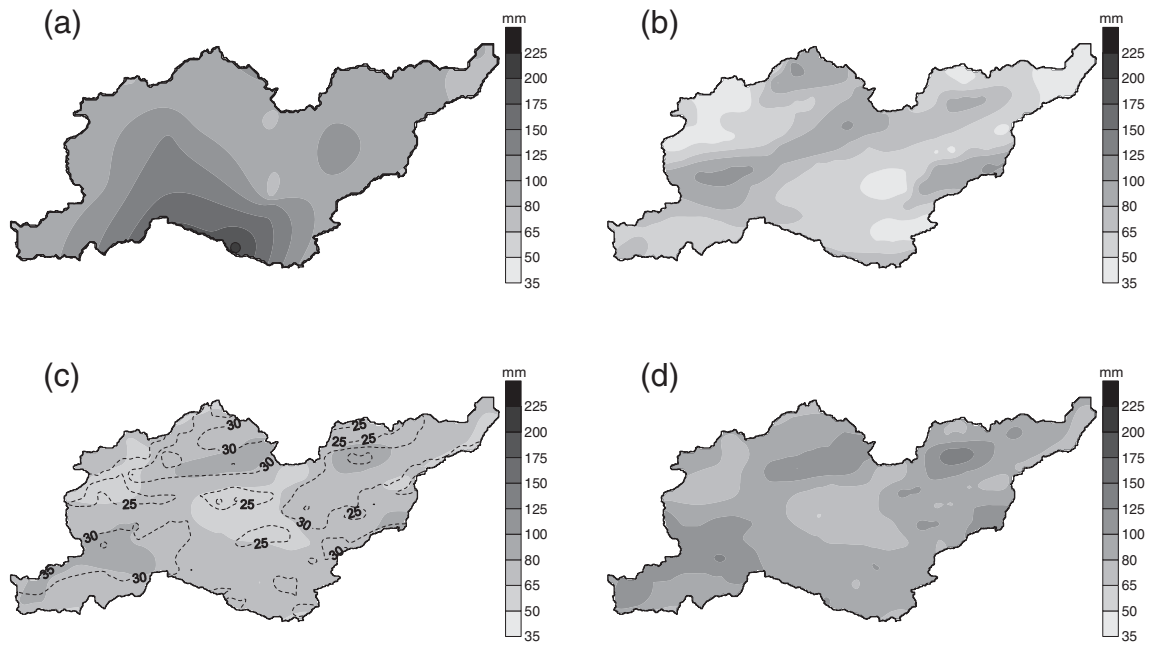


Fig. 6. Accumulated precipitation in the Guadalentín river basin from 27 to 28 September 2012 00 UTC according to (a) rain-gauges and WRF (b) control, (c) ensemble mean and (d) probability-matched ensemble mean experiments. Ensemble standard deviation also shown as dashed lines for the ensemble mean (in mm, starting at 20 mm and at 2.5 mm intervals).

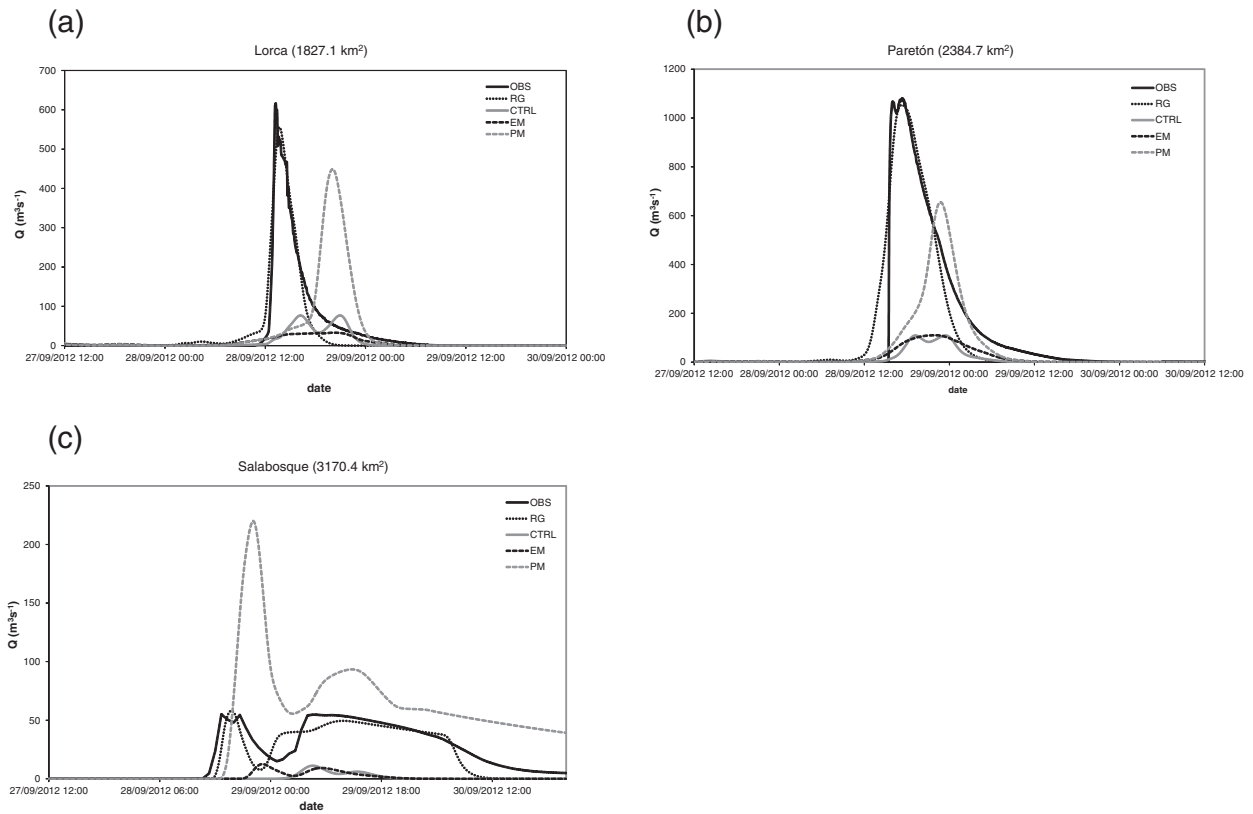


Fig. 7. Observed (OBS), rain-gauge (RG) and WRF control (CTRL), ensemble mean (EM) and probability-matched ensemble mean (PM) driven runoff simulations for the 28 September 2012 episode at (a) Lorca, (b) Paretón and (c) Salabosque flow-gauges.

3170.4 km² at Salabosque, where the last flow-gauge is installed (Fig. 2). The model determines runoff volumes by subtracting the water volume lost through interception, infiltration, storage and evapotranspiration from hourly rainfall. The loss rate is calculated using the Soil Conservation Service-Curve Number (SCS-CN; US Department of Agriculture, 1986). This method assumes the storm runoff volumes to be proportional to the rainfall volumes exceeding an initial abstraction threshold (I_a), through the ratio of the accumulated infiltration to a storage capacity. With this assumption and according to the continuity principle, the cumulative volume of storm flow becomes non-linearly related to the excess rainfall volume, which is a function of cumulative rainfall, soil cover, land use and antecedent moisture (Chow et al., 1988). The SCS-CN model has been tested on several experimental areas and river basins worldwide (Ranzi et al., 2003; Amengual et al., 2007; Borga et al., 2007; Rabuffetti et al., 2008). A synthetic unit hydrograph provided by SCS (SCS-UH) is used to convert rainfall excess into direct runoff on a watershed. The SCS-UH relates the peak discharge with the time to the peak through the sub-basin area and a conversion constant. The flood hydrograph is routed using the Muskingum method (Chow et al., 1988; USACE-HEC, 2000).

The Guadalentín contains four reservoirs. *Valdeinferno*, *Puentes* and *Algeciras* are located in the upstream mountainous areas of the main river tributaries and are used for water supply and flood control. The *José Bautista* dam is situated into the river valley and is only used for flood control purposes (Fig. 2). The reservoirs are modeled by using the elevation–storage–outflow relationship series. This relationship depends on the characteristics of the dam, the outlet and the spillway, and on the initial elevation of the water level (USACE-HEC, 2000). The initial elevations have been obtained from the CHS database for the 00 UTC 27 September to 00 UTC 01 October 2012 period. Storage capacities, maximum outflows and maximum water elevations have been provided by the CHS hydraulic division. In addition, a diversion element has been introduced downstream of Paretón de Totana to account for the

redirected discharges towards the Mediterranean Sea. Diverted flows for the simulation period have been obtained from the CHS database as well.

4.2. Input data and basin calibration

The hydrological model is forced by using a single hyetograph for each sub-basin. Rainfall spatial distributions are first generated from hourly accumulated values recorded at the automatic rain-gauges by applying the kriging interpolation method with a horizontal grid resolution of 500 m. Then, the hourly rainfall series are calculated for each sub-basin as the area-averaged of the gridded rainfall within each sub-catchment. The same methodology is applied to force HEC-HMS with QPFs, but by using gridded WRF forecasts instead. Kriging relies on the application of a linear model for the variogram fit. This minimal error variance method is recommended for irregular observational networks and has been commonly used to compute rainfall fields from rain-gauges (Krajewski, 1987; Bhagarva and Danard, 1994; Seo, 1998).

Curve numbers have been extracted from previous flood risk assessment tasks carried out by the regional government of Murcia (INUNMUR, 2007). SCS-CN_s were initially derived from field measurements and by considering normal antecedent moisture conditions (i.e. total 5-day antecedent rainfall between 12.7 and 27.9 mm). However, the summery conditions prior to the 28 September 2012 flash-flood resulted in low soil moisture content and high initial abstractions. Therefore, SCS-CN_s and I_a _s have been considered as calibration indices after this long hot and dry period. Both parameters have been shown to exercise a dominant role on extreme flood response over the semi-arid Mediterranean Spain (Amengual et al., 2007). In addition, large and intense convective precipitations during late summer quickly exceed the infiltration capacity of the dry soils, generating fast Hortonian flows. High overland flows result in a systematic decrease of basin response owing to the expansion on stream network to unchanneled topographic elements for

the hillslopes (Borga et al., 2007). Accordingly, lag time (T_r) for the basins receiving large rainfall accumulations has been subject to calibration as well. Finally, the flood wave celerity for the main streams – by means of the K parameter – has been calibrated, as these extremes feature very high flow velocities (Amengual et al., 2007). Calibration tasks have combined a manual and an automated procedure. The latter uses the peak-weighted root mean square error as an objective function and applies the univariate-gradient search algorithm method (USACE-HEC, 2000).

Calibration has been performed with observed rainfall accumulations and stream-flows of this event, thus using the perfect-model assumption to evaluate deterministic and probabilistic QPFs. That is, we assume that a perfect set of parameters optimizing the rainfall-runoff model performance before this extreme flood has been found after calibration (Table 1). Under this assumption, errors in the predicted stream-flow will be attributed to deficiencies in the QPFs. Thus, we focus our analysis on the impacts that synoptic-scale uncertainties in the meteorological model initial conditions produce in the stream-flow forecast, minimizing the impact of other sources of uncertainty such as meteorological and hydrological model errors or the link between both modeling systems. The whole set of hydrological simulations has been run for a 96-hour period, from 00 UTC 27 September to 00 UTC 01 October 2012, with a 5 minute time-step. This period safely encompasses the primary flood event and the subsequent hydrograph tail. Note that the HEC-HMS linearly interpolates hourly precipitation to its computational time-step.

5. Meteorological tools

Accurate numerical simulation of deep moist convection and extreme precipitation rates is difficult owing to the highly nonlinear character of the schemes representing the physical processes leading to their formation. Not only is the parameterization of physical processes inexact, but any misrepresentation of the atmospheric state across the relevant scales strongly penalizes the forecast quality in such nonlinear systems (Toth and Kalnay, 1993; Mullen and Baumhoffer, 1988; Houtekamer and Derome, 1995; Du et al., 1997). Indeed, errors of any origin can grow rapidly during the forecast and lead to inaccurate predictions. The ECMWF produces an ensemble of global forecasts with the aim of sampling the distribution of plausible atmospheric states, given the bulk of observational and modeled information available (Buizza and Palmer, 1995; Molteni et al., 1996). In particular, the ECMWF global ensemble prediction system consists of 50 members generated by perturbing an analysis with the singular vector technique. Branković et al. (2008) showed that the high-resolution simulated precipitation rates and patterns were improved with respect to the global forecasts mainly owing to the more accurate simulation of sub-synoptic scales. Marsigli et al. (2005) not only showed the benefit of large ensemble sizes, but also confirmed the improvement of the high-resolution limited-area model in the forecast of heavy precipitation, diminishing the importance of the role of physical parameterizations with respect to the initial and boundary conditions when accounting for relevant sources of uncertainties in the forecast of flood events in the Western Mediterranean.

Based on these findings, we explore the ability to produce reliable precipitation forecasts of an ensemble of mesoscale numerical simulations forced by the 51 members of the global T639L62 ECMWF EPS, including control run. We generate a high-resolution EPS with a large number of ensemble members to encompass better any possible issues

Table 1

Sub-basin average of hydrological model parameters before and after calibration tasks. Also shown are standard deviations in brackets.

Parameter	SCS-CN	I_a (mm)	T_r (h)	K (h)
Before	71.7 (1.6)	20.1 (1.6)	2.2 (0.4)	2.7 (1.5)
After	69.2 (4.1)	73.0 (22.6)	2.0 (0.5)	2.4 (1.5)

of underdispersion (Cloke and Pappenberger, 2009; Clark et al., 2011). The dynamical downscaling is performed with the WRF3.4 model with 4 km grid spacing, 28 vertical levels, and a domain that covers the Western Mediterranean, as it is routinely used in the Group of Meteorology at the University of the Balearic Islands (Fig. 1; see <http://meteo.uib.es/wrf>). The physical parameterizations used are identical in all 51 simulations and include: the WRF single-moment 6-class microphysical scheme incorporating graupel (Hong and Lim, 2006); the 1.5-order Mellor–Yamada–Janjic boundary layer scheme (Janjic, 1994); and the new Kain–Fritsch cumulus scheme (Kain, 2004). Simulations were run for 48 h from 00 UTC 27 to 00 UTC 29 September 2012, encompassing the initiation phase and the mature evolution of the most active convective systems along the Spanish Mediterranean coast. Eventually, a regional downscaled ensemble prediction system based on WRF runs (WEPS) produces an ensemble of hourly QPFs that are fed into the hydrological model to generate a HEPS.

6. Results

6.1. Rain-gauge driven runoff simulation

As a safety check, we assess the ability of the hydrological model to reproduce the 28 September 2012 observed stream-flows in the Guadalentín river basin when driven by rain-gauge precipitation measures. Since we are interested in analyzing the predictability of the QPF at basin scale, we evaluate the deterministic and probabilistic hourly accumulations over the Guadalentín catchment. The performance of the rain-gauge driven runoff simulation is expressed in terms of the Nash–Sutcliffe efficiency criterion (NSE; Nash and Sutcliffe, 1970) and the relative percentage errors of the total volume (%EV) and peak discharges (%EP) at the flow-gauge sites. Once calibrated, the rainfall-runoff model accurately reproduces the hydrological response of the basin in terms of the observed peak discharges and runoff volumes. NSE exceeds 0.8 at Salabosque flow-gauge and slightly overpasses 0.9 at Lorca and Paretón hydrometric sections (Table 2, Fig. 7). For the latter, only minor underestimations of the runoff volumes are found. The times of peak discharge are also well simulated; only a moderate error in timing is found at Lorca. The goodness of fit for the main peak discharges become evident, even if the calibrated run only simulates an envelope of the two high-frequency observed peaks at Paretón and Salabosque. It is noteworthy the extremely steep slopes of the rising limbs for the observed hydrographs, denoting the extraordinary increases in the flow discharge rates (Fig. 7). These results point out the effective adjustment of the model's initial and dynamical formulation parameters. The hydrological response of the Guadalentín basin to the extreme flood can be well simulated by HEC-HMS when driven by rain-gauge data spatially interpolated and when correctly and fully calibrated. Therefore, subsequent deterministic and probabilistic driven runoff experiments can be safely carried out under the hydrological perfect-model assumption.

6.2. WRF driven runoff simulations

In this section, we analyze the predictability of the streamflow for this flash-flood. QPFs are examined against the rain-gauge rainfall patterns by using the 27 sub-basins as hourly rainfall accumulation

Table 2

NSE efficiency criterion, percentage of error in volume (%EV) and peak flow (%EP) for the rain-gauge driven and WRF control driven runoff simulations at the indicated sites.

Flow-gauge	NSE	% EV	% EP	NSE	% EV	% EP
	RG	RG	RG	WRF control	WRF control	WRF control
Lorca	0.93	–8.2	–10.0	0.13	–73.2	–87.5
Paretón	0.91	–5.7	–2.6	0.12	–88.4	–89.9
Salabosque	0.84	–16.3	5.3	–0.64	–94.9	–79.7

units. To this end, hourly QPFs volumes are compared against the hourly rain-gauge volumes for all the sub-basins. The temporal distributions are also computed through the hourly rainfall volumes, but over the whole catchment. QDFs coming from forcing the hydrological model with WRF outputs are compared against the rain-gauge driven runoff simulation as well. We compare the spatial and temporal distributions of the QDFs against the rain-gauge driven runoff simulation by applying the same procedure as when evaluating QPFs, but using the sub-basins as hourly runoff accumulation units instead.

6.2.1. Deterministic QPFs driven runoff simulations

The correlation coefficient (*r*) and mean absolute (MAE) and root-mean-squared (RMSE) errors are used for evaluating the skill of the control, ensemble mean and probability-matched ensemble mean QPFs (Jolliffe and Stephenson, 2003; Wilks, 2006). Keep in mind that the ensemble mean provides a better forecast than any individual ensemble member only for a large sample size, because errors in the individual forecasts tend to cancel when significantly averaged (Epstein, 1969; Leith, 1974). However, the ensemble mean is still devotedly exploited for certain deterministically-oriented end-users, even when these are very sensitive to extreme events (Junker et al., 2009). Admittedly though, the ensemble mean is likely to forecast the general location of the maximum precipitation amounts best as small scale variability present in individual members is effectively averaged out. Thus, WEPS ensemble mean precipitation and the derived runoff volumes are computed in order to highlight the possible benefits of a simple ensemble average against the control experiment. However, ensemble mean precipitation rates are smoothed out and maximum rainfalls are accordingly reduced. The amounts of the observed precipitation rates are usually better forecast by individual members. With the aim of accounting for this effect, Ebert (2001) introduced the probability-matched (PM) ensemble mean, which transforms the rain rate distribution in the ensemble mean to resemble that of the complete ensemble. That is, PM ensemble mean has the spatial distribution of the ensemble mean, but the precipitation amounts reproduce the distribution of the ensemble members. Therefore, probability matching renders more realistic precipitation amounts than the plain ensemble mean field.

Regarding the control experiment, the maximum precipitation amounts are reasonably well reproduced over southern Murcia and Valencia, but are mainly distributed over a maritime strip along their coastlines (Fig. 5). Over the Guadalentín basin, total rainfalls underestimate the maximum observed amounts in the southern part (Fig. 6). The ensemble mean shows maximum amounts distributed over the Baetic system and along the coast of Murcia (Fig. 5). Even if the location of precipitation maxima is better predicted with respect to the control run, these barely reach 100 mm. Conversely, the PM ensemble mean shows maximum values significantly higher than the bare ensemble mean and the areas comprising heavy precipitations are more extensive, including the Guadalentín basin (Fig. 6). Although the 48 h accumulated volumes over the sub-basins show high correlation with observations, RMSE and MAE penalize the above mentioned inaccuracies (Table 3). Temporal correlations result weaker than the spatial correlations owing to the significant underproductions of the hourly rainfall volumes. The ensemble mean neither reproduces the observed

maximum cumulative amounts nor the rates of precipitation at the catchment scale. On the other hand, the PM ensemble mean reproduces the extreme precipitation, even if a 3–4 h delay results in lower temporal correlations, yielding the lowest score of the whole set of deterministic experiments (Table 3). Note the negative impact on the spatial skill scores that increased hourly rainfall amounts produced when compared to the ensemble mean, even though the spatial patterns are identical. PM ensemble mean driven runoff experiment is the best deterministic prediction in terms of precipitated water and runoff volumes (Tables 2 and 4). The main inaccuracies arise from an underestimation of the rainfall amounts over the upper and middle parts of the basin. So, the PM driven peaks discharges are lower than the rain-gauge driven maximum flows at Lorca and Paretón (Figs. 6 and 7). Downstream of the diversion – where most of both flow volumes are redirected to the Mediterranean Sea, the overproduction of the PM rainfall amounts over the lower part of the catchment results in higher peak flows than the rain-gauge maximum discharges. Errors in the remaining deterministic QPFs strongly propagate through the hydrometeorological chain. That is, the control and ensemble mean driven runoff simulations neither capture the observed peak discharges nor the total runoff volumes, resulting in a complete miss of the flash-flood (Table 2; Fig. 7). The high non-linearity in the hydrological response – related to threshold effects on runoff production – produces a clear degradation of the QDF forecasting skills (Table 4). These limitations have arisen as much of the small-scale information of the WEPS precipitation rates has been averaged out by the ensemble mean strategy. On the contrary, the PM ensemble mean approach partially copes with these problems, yielding more realistic maximum precipitation rates.

6.2.2. Probabilistic QPF driven runoff simulations

Here, we assess the added value of a probabilistic approach with respect to these deterministic products at guiding and supporting short-range hydrometeorological warning chains. Admittedly, the computation of probabilistic verification scores from a single extreme flood event is challenging and its significance is limited. Nevertheless, computing those scores is useful to understand better the behavior of the studied ensemble and to highlight its strengths and weaknesses. This research is not aimed at computing verification scores for a certain HEPS configuration, but at exploring the potential of the proposed HEPS to support decision makers dealing with civil protection and emergency management before such extremes.

A set of categorical verification scores has been employed to evaluate probabilistic QPFs and QDFs (PQPFs and PQDFs) against the rain-gauge rainfall and driven runoff volumes. These scores provide information on the general performance of the WEPS and HEPS to forecast the rainfall and runoff volumes at the basin scale. Specifically, performance has been assessed through the Brier (BS) and Relative Operating Characteristic (ROC) scores, as well as through a set of graphical representations of probabilities as the reliability, sharpness and Talagrand diagrams (Jolliffe and Stephenson, 2003; Wilks, 2006). These statistical scores are computed for specified thresholds of PQPF and PQDF volumes (i.e. V_p, V_q , respectively). These forecast probability levels are: $V_p, V_q < 0.05$; $0.05 \leq V_p, V_q < 0.15$; $0.15 \leq V_p, V_q < 0.25$; ...; $0.85 \leq V_p, V_q < 0.95$; and $V_p, V_q \geq 0.95$. WEPS and HEPS are verified for the following hourly volume thresholds: 2, 4, 8, 16, 32 and 64 ($\cdot 10^3$) m^3 . Note that the observed sample size is of $N = 1296$ (48 time-steps \times 27 sub-basins)

Table 3
Correlation coefficient, RMSE (in $\cdot 10^6 m^3$) and MAE (in $\cdot 10^6 m^3$) of the hourly spatial and temporal rainfall volume distributions yielded by the WRF control, ensemble mean and probability-matched experiments. Note that the spatial accumulations have been computed at sub-basin scale, while the temporal accumulations have been calculated at basin scale.

Experiment	<i>r</i>	RMSE	MAE	<i>r</i>	RMSE	MAE
	Spatial	Spatial	Spatial	Temporal	Temporal	Temporal
Control	0.86	5.19	4.36	0.51	12.40	6.42
Ensemble mean	0.90	4.51	3.77	0.63	11.04	6.03
Probability-matched	0.82	5.42	4.25	0.48	14.05	7.38

Table 4
Ratio to the total rain-gauge rainfall and driven runoff volumes over the Guadalentín catchment for the control, ensemble mean and probability-matched experiments. Note that rain-gauge rainfall and driven runoff volumes are of 329.4 and 37.2 ($10^6 m^3$), respectively, which correspond to a runoff ratio of 0.11.

	Control	Ensemble mean	Probability-matched
Rainfall	0.64	0.69	1.16
Runoff	0.10	0.14	1.45

and of $N = 2592$ (96 time-steps \times 27 sub-basins) for the rainfall and runoff volumes, respectively. Admittedly, among-sample correlations within subsets of observed precipitation could be present due to coherent spatial patterns. Given the spatial and temporal variability of the precipitation fields, this fact is assumed to have little impact on the verification scores.

The translation of synoptic-scale ECMWF-derived uncertainties in the WRF model initial conditions to basin-averaged cumulative precipitations (Fig. 8) is a first indication of the great potential of the proposed forecasting design. The large ensemble spread points out the limited predictability of such small-scale predictand both in terms of accumulations and timing of the most intense rainfall rates. Despite that none of the numerical predictions simulates the high precipitation rates as early on 29 September as those observed, a number of WEPS members pick this feature up shortly afterwards (from 06 to 12 UTC). Regarding the accumulated amounts, the benefits of using a probabilistic prediction system emerge very explicitly. Not only accounting for uncertainties in the forecasting system provides indications of plausible scenarios with much higher accumulations than the deterministic control run, but also allows for the calculation of probabilities of exceedance for certain critical thresholds for civil protection protocols. Fig. 8 evidences the wealth of valuable information about the possible scenarios compatible with the uncertainties of the day that is ignored when just considering deterministic products as control or ensemble mean experiments.

Table 5 and Fig. 9a show that accuracy of probability forecasts is relatively high and it increases at high volume thresholds as a natural consequence of having low probabilities for simulating and observing extremes. The best reliability scores are obtained for the higher precipitation volume thresholds which generally tend to have more slope, but at the expense of resolution. In general, the reliability diagram shows an over-confident WEPS, with under-prediction of low probability levels and over-prediction of high probability forecasts (Fig. 9b). Note that the reliability curves are not monotonic, hampering a possible calibration of the WEPS probabilistic output. The sharpness diagram confirms that each forecast probability bin is well populated (Fig. 9b). As a consequence of the sub-basin evaluation of these scores, the Talagrand diagram shows an underdispersive ensemble, mostly attributable to the time lag in the WEPS predictions of intense precipitation rates (Fig. 8). This temporal lag causes frequent observed accumulations laying outside the predicted range. However, the predictions still hold considerable information for the end-user, even including dispersion.

Fig. 10 depicts the distribution of plausible run-off levels in the Guadalentín basin for this episode as predicted by our HEPS. At all

Table 5
ROC scores for the forecast probabilities of the ensemble members at different hourly rainfall and runoff volume thresholds.

Thresholds (in $\cdot 10^3 \text{ m}^3$)	ROC rainfall	ROC runoff
2	0.797	0.785
4	0.784	0.779
8	0.776	0.756
16	0.774	0.742
32	0.773	0.727
64	0.765	0.727

stream-gauges, the ensemble median is very similar to the control driven runoff simulation, resulting in discharges far below and temporally shifted from the reference raingauge-driven predicted flow. Conversely, the HEPS results are encouraging in terms of support providers for civil protection management systems. Admittedly, the Salabosque prediction would have produced excessive false alarm and the predictions in the other two stations are far from perfect. However, societal tolerance to false alarms is larger than to misses owing to the damaging impacts of these extreme events. Eventually, the single inclusion in the forecasting chain of synoptic scale uncertainties in the precursing conditions of this catastrophic flood is proved sufficient to predict a scenario with extreme predicted stream-flows throughout the basin, despite the low estimated level of predictability – as revealed by the dispersion in Fig. 10.

Fig. 11a reveals that the magnitude of the probability forecast errors is low for the PQDFs. The best reliability and resolution scores are obtained at low runoff volumes. That is, the HEPS discriminates better whether low runoffs occur than for higher stream-flows. The reliability diagram depicts important overforecasting probability biases for this extreme flooding (Fig. 11b). The sharpness diagram points out that the majority of PQDFs features low probabilities for the outer-quintile categories, and the HEPS is not able to predict relatively high probabilities (Fig. 11b). The rank histogram indicates a low bias: frequencies are lower than expected for small runoff volumes and higher than expected for high discharge volumes (Fig. 11d). That is, HEPS features a systematic dry bias as shown by the left skewness of the Talagrand diagram. Finally, as all ROC scores are well above 0.5, the discrimination ability of the EPS and HEPS is useful (Table 5; Fig. 12). That is, the ROC areas render an unbiased and unhedged estimate of the ensemble resolution.

6.2.3. The probabilistic hydrometeorological forecasting chain

As shown, the challenging task of reproducing the precise location, timing and rainfall amounts associated with localized MCSs affecting

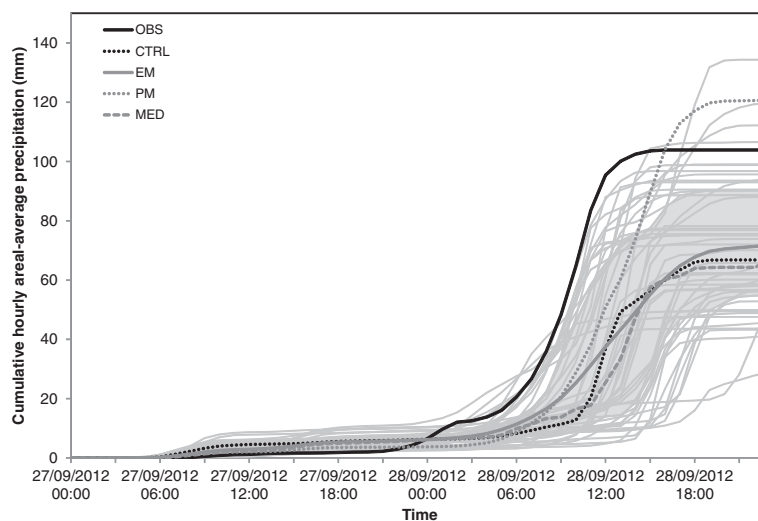


Fig. 8. Cumulative hourly areal-averaged rainfall amounts over the Guadalentín river basin for the ensemble members from 27 to 29 September 2012 00 UTC. Ensemble members are shown as thin gray lines. Observed (OBS), control (CTRL), ensemble mean (EM), probability-matched ensemble mean (PM) and the ensemble median (MED) cumulative hourly areal-averaged values are also displayed. The shaded area represents the interquartile (q25–q75) range.

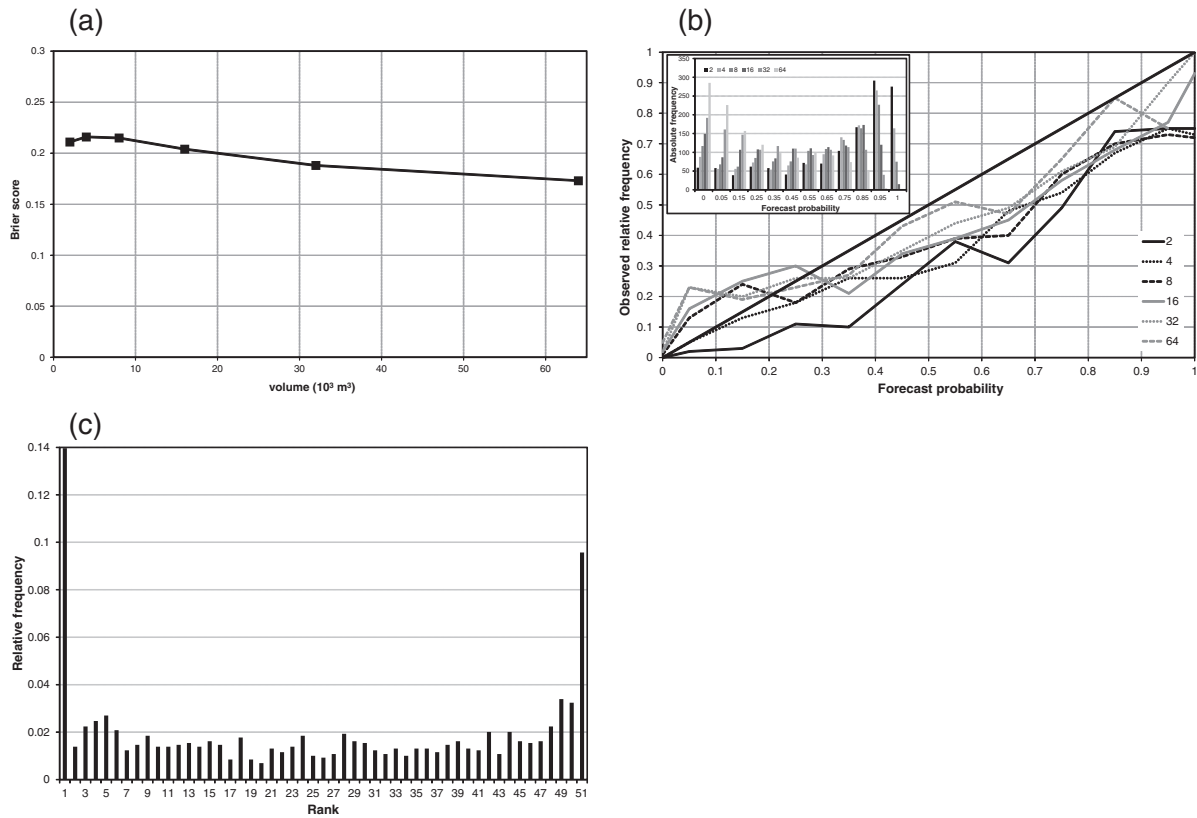


Fig. 9. Brier score (a), and reliability and sharpness diagrams (b) for different precipitation volume thresholds obtained by the ensemble members. The Talagrand diagram (c) is also shown. Note that the labels of the reliability and sharpness diagrams denote the different precipitation volume thresholds (in $\cdot 10^3 \text{ m}^3$).

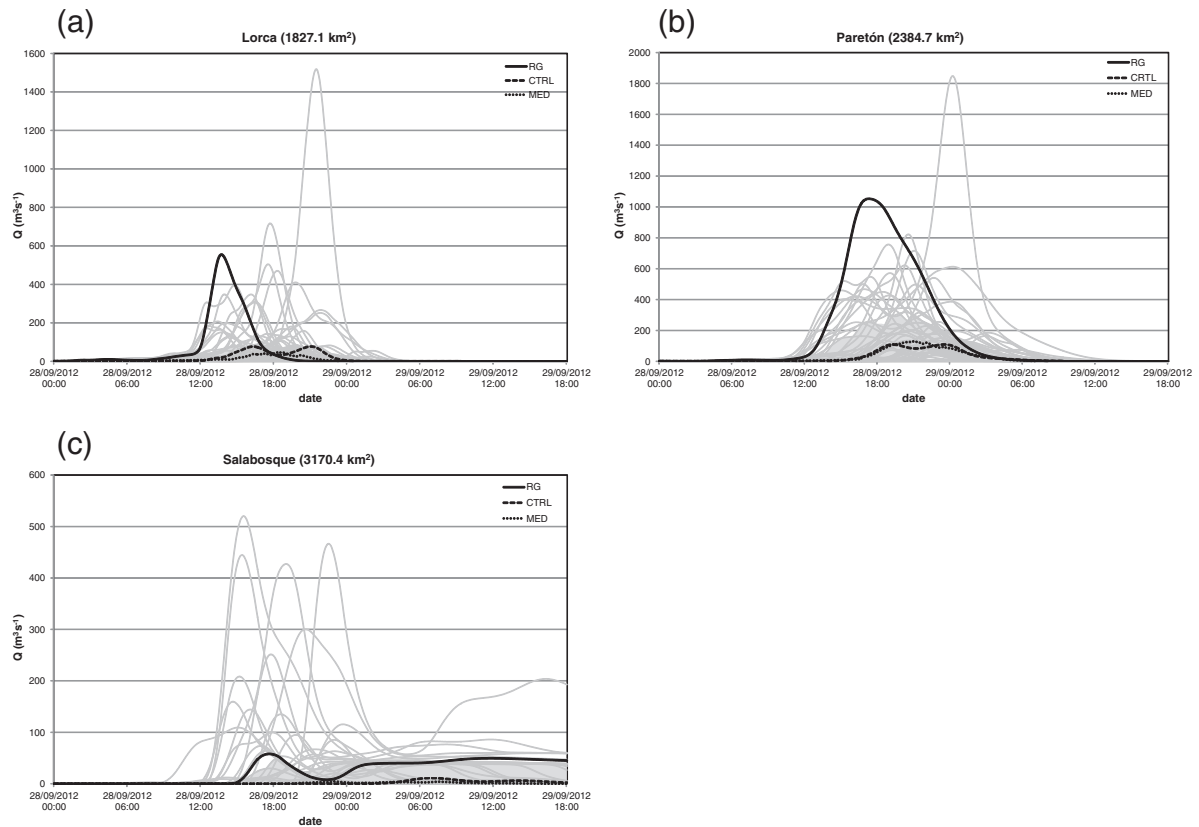


Fig. 10. Rain-gauge (RG), control (CTRL) and ensemble median (MED) driven runoff simulations for the 28 September 2012 episode at (a) Lorca, (b) Paretón and (c) Salabosque flow-gauges. The shaded area represents the interquartile (q25–q75) range.

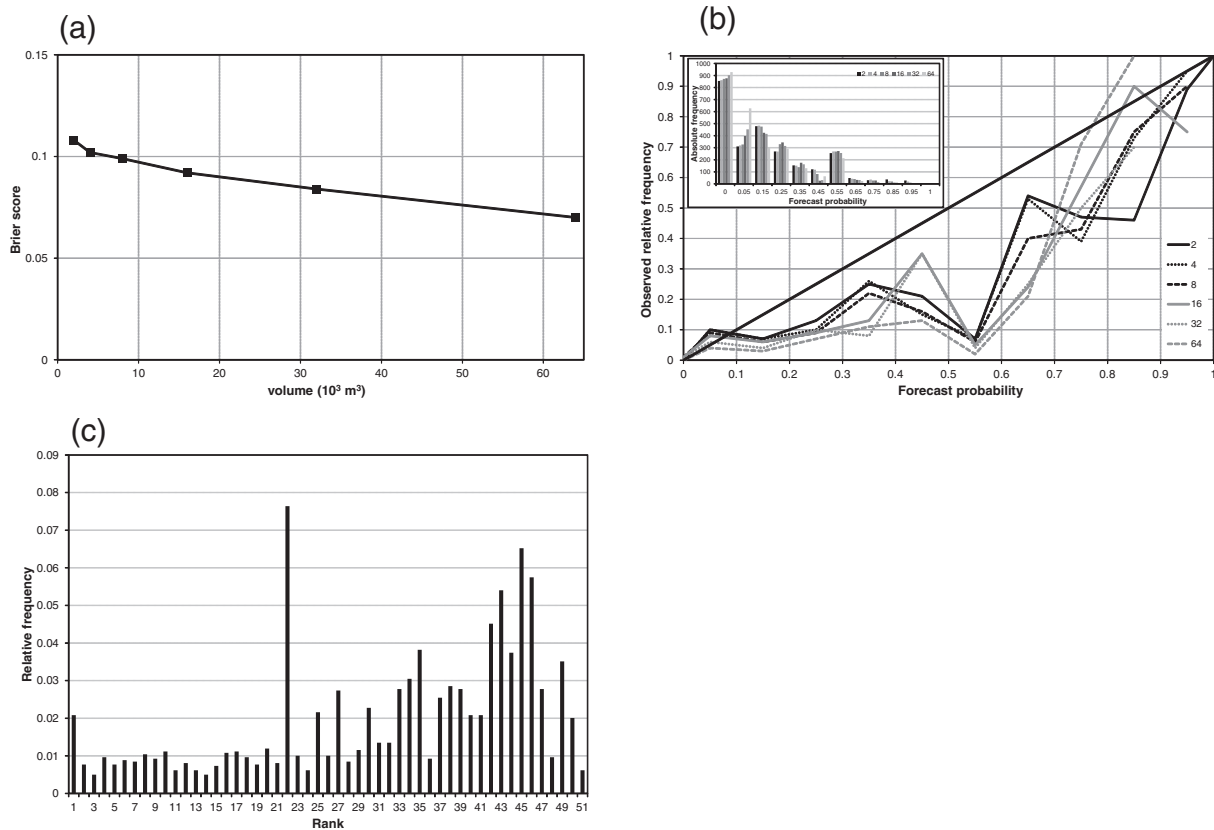


Fig. 11. As in Fig. 9, but for different runoff volume thresholds obtained by the ensemble of WRF driven runoff simulations.

small- and medium-sized basins represents an obstacle that most times is only possible to overcome by using advanced HEPS. In fact, inaccuracies in the control QPFs at forecasting the heavy rainfall-bearing convective cells would have prevented the triggering of any flood warning for this flash-flood. To obtain some insights into the performance of an experimental probabilistic flood prediction chain when dealing with extreme discharges, we include this case study demonstration. No real-time hydrometeorological forecasting chain is currently implemented for civil protection purposes in the Guadalentín river basin. Within a civil protection framework, a warning should be issued whenever the HEPS peak discharges exceed pre-determined thresholds at the hydrometric sections of interest. To this end, we consider two hypothetical warning discharge thresholds, corresponding to the maximum peak discharges for different return periods ($Q_{p(T)}$; INUNMUR, 2007). We consider $Q_{p(T=25 \text{ years})} = 115.0 \text{ m}^3 \text{ s}^{-1}$ and $Q_{p(T=35 \text{ years})} = 238.5 \text{ m}^3 \text{ s}^{-1}$ at Lorca and Paretón. At Salabosque, $Q_{p(T)}$ s are of $172.6 \text{ m}^3 \text{ s}^{-1}$ and $511.9 \text{ m}^3 \text{ s}^{-1}$ for $T = 10$ and $T = 20$ years, respectively.

HEPS peak flows have been represented as cumulative distribution functions (CDFs) plotted on a Gumbel chart (Fig. 13; Ferraris et al., 2002; Amengual et al., 2008, 2009). At Lorca and Paretón, little differences are found between the control and ensemble median peak discharges. However, biases in the deterministic experiment are somewhat alleviated by using a HEPS strategy, as some ensemble members reasonably forecast the observed extreme peaks. Although the peak discharge exceedance probabilities for the observed maximums are below 0.1, $Q_{p(T=25 \text{ years})}$ and $Q_{p(T=35 \text{ years})}$ are close to 0.4 and 0.25, and to 0.7 and 0.45 at Lorca and Paretón, respectively. In addition, the ensemble spread encompasses both thresholds at these hydrometric sections. At Salabosque, many of the HEPS peaks overforecast the maximum observed flow ($P[Q \geq q] = 0.37$). This fact highlights the importance of having precise information on the location of the maximum forecast rainfall amounts when dealing with a highly human-modified river basin. As numerous water supply and flood control facilities are

deployed in the Guadalentín river basin, even small errors on the location of the actual maximum precipitation amounts – slightly up or downstream of a reservoir or the diversion channel – have an important impact on the flow outcomes (Figs. 10c and 13c). Thus, it becomes evident that a probabilistic strategy provides more useful information when compared to a deterministic approach.

PQDFs for emergency management purposes may not need to match exactly the peak discharges or the timing, but must reach suitable thresholds to enact the appropriate protocols (Ferraris et al., 2002; Amengual et al., 2009; Vincendon et al., 2011; Addor et al., 2011). From a civil protection perspective, a warning should be issued whenever the forecast peak discharges exceed pre-determined thresholds at the hydrometric sections. For instance, the Spanish Agency of Meteorology (AEMET) issues a warning when the probability of occurrence of an extreme event exceeds 0.2. Following this criterion, an early issuance of warnings for the 28 September 2012 flash-flood would have been possible, even if the exact magnitude may have been missed. On the contrary, analogous deterministic QDFs would not have enacted the triggering of any warning.

7. Conclusions and further remarks

The HyMeX program devotes special attention to the extreme hydrometeorological events affecting the Western Mediterranean region and aims at providing a tangible basis for flood early warning procedures and mitigation measures. In the Mediterranean Spain, most extreme flash-floods are associated with quasi-stationary and small-sized MCSs, causing substantial flood damage. Any kind of gain in runoff forecast accuracy and lead times can be used to improve warning and emergency procedures in order to alleviate possible social impacts. HEPSs are nowadays being tested in order to quantify their added value on top of deterministic runoff forecasts when extending lead times beyond the concentration time of small- and medium-sized

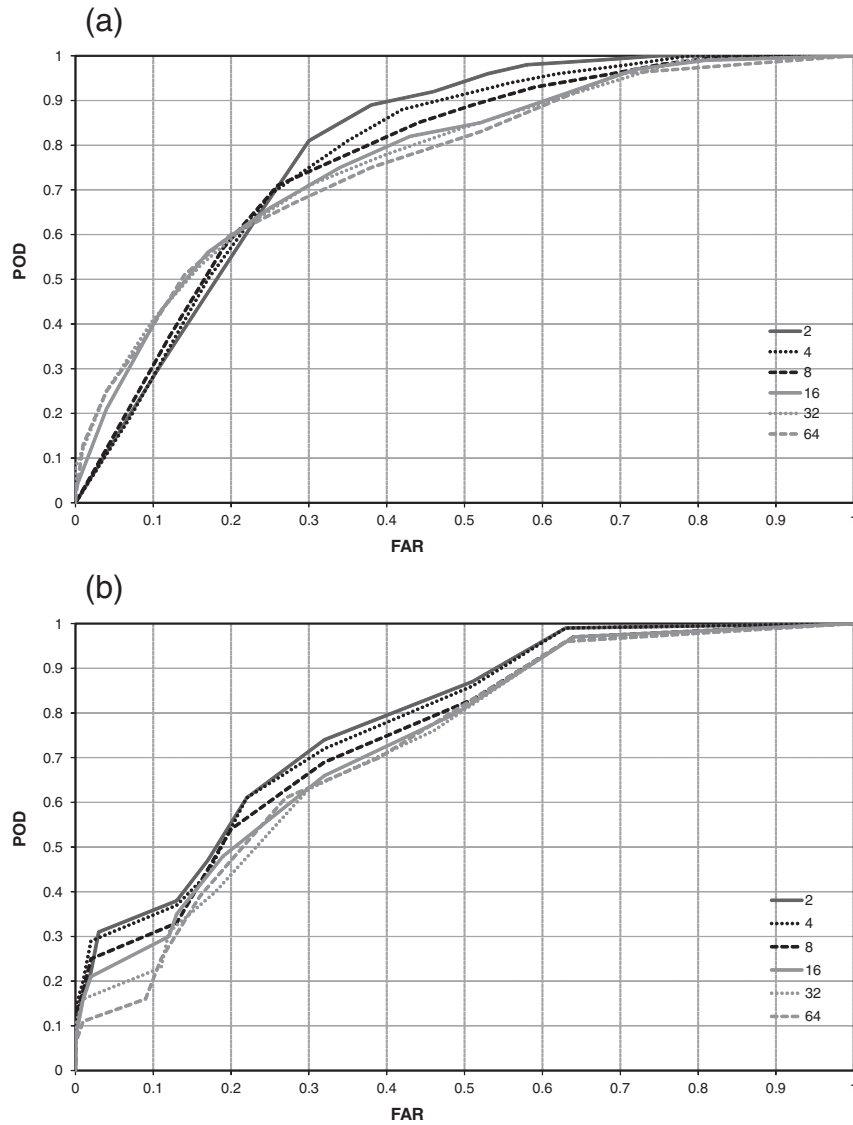


Fig. 12. ROC scores of the forecast probabilities for the ensemble members at different hourly (a) rainfall and (b) runoff volume thresholds (in $\cdot 10^3 \text{ m}^3$).

watersheds. The exploitation of the warn-on-forecast concept for hydrological prediction is an essential task when dealing with such extremes over the flood-prone Spanish Mediterranean area.

To this end, deterministic and probabilistic QPFs have been obtained by downscaling the global ECMWF-EPS forecasts over the region with the high-resolution limited-area WRF model. The ensemble strategy is designed to account only for uncertainties coming from the atmospheric precursing conditions, allowing to study their impact on the HEPS predictions. When evaluating the QPFs, the one-way coupling between the meteorological and calibrated (i.e. assumed perfect) hydrological model is used as an advanced and user-oriented verification tool. That is, the integrating effect of the catchment surface copes with the high spatial and temporal variability of extreme convectively-driven precipitation. Since small-scale and intense cores of precipitation limit the accuracy of evaluating QPFs from sparse rain-gauge networks, the streamflows estimate better the amount of precipitated water over the basin.

Deterministic QPFs have shown significant deficiencies in terms of precipitation rates, their location and timing over the Guadalentín river basin. Subsequent QDFs have enhanced biases found in QPFs as a consequence of the high non-linearity in the hydrological response related to threshold effects. Inaccuracies in atmospheric initial conditions

are reflected through moderate spatial and temporal variations of the QPFs as well as in significant changes of the precipitation rates and total amounts at basin scale. Even if the predictability of the 28 September 2012 extreme episode remains limited, the HEPS has partially coped with these biases. PQDFs would have indicated exceedance of a set of pre-defined warning thresholds within a probabilistic hydrological forecasting chain, thus providing a useful basis for flood early warning procedures and mitigation measures. Therefore, it is clear the added value conveyed by an ensemble strategy when compared against a deterministic forecasting approach for warning and emergency purposes.

However, the reliability and skill of the hydrological model must be improved in the framework of an actual hydrometeorological forecasting configuration. For instance, the lack of streamflow data for similar past hydrometeorological events over the Guadalentín river basin has prevented to carry out broader calibration and verification tasks. Hydrological model parameters – related to the initial conditions and channel routing – has been just assessed for this extreme episode. That is, the rainfall–runoff model has been run under a best estimation of the parameters for the infiltration and dynamical processes for the 28 September 2012 flash flood. As we rely on a single case study, subsequent evaluation of the HEPS is somewhat limited and results should be

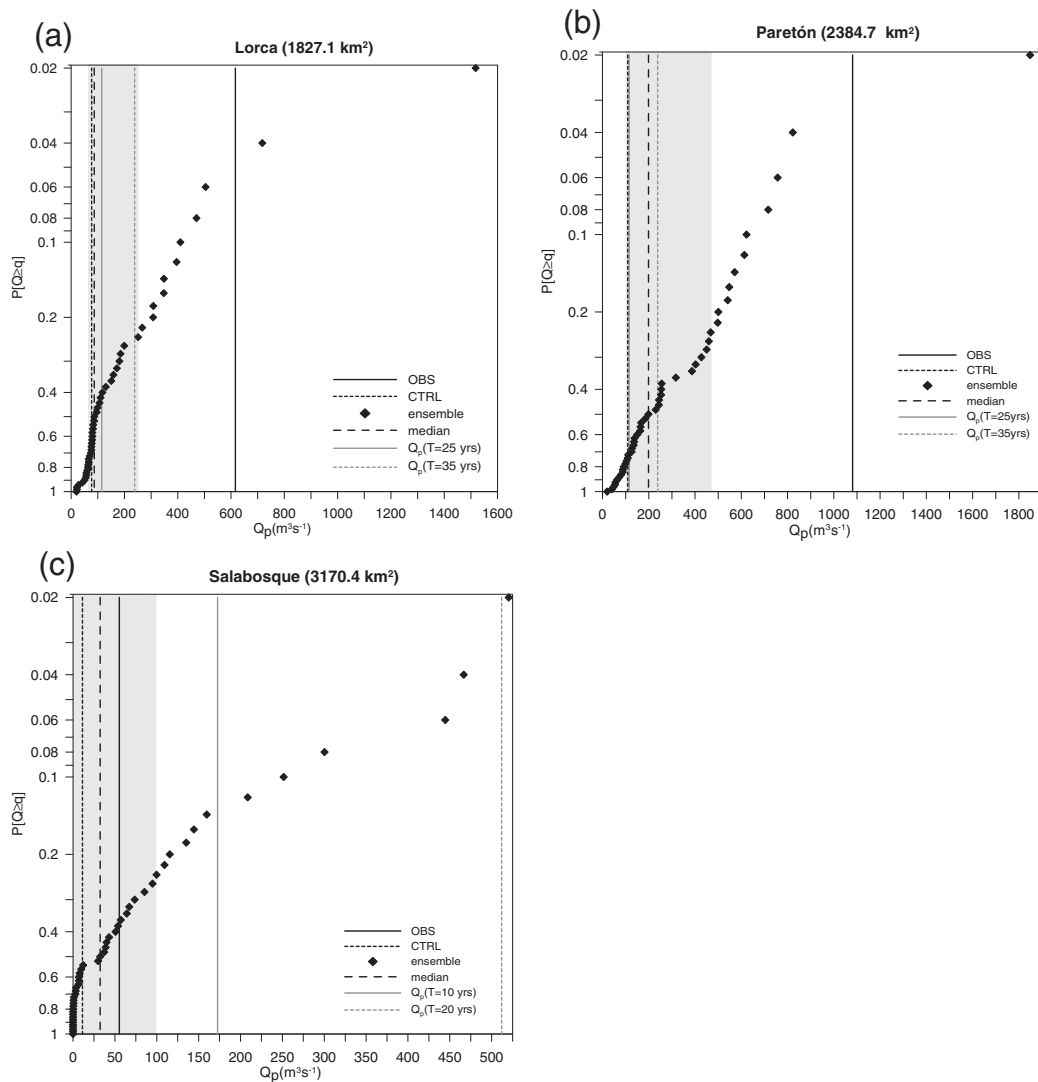


Fig. 13. Peak discharge exceedance probabilities for the 28 September 2012 hydrometeorological episode at (a) Lorca, (b) Paretón and (c) Salabosque flow-gages. The vertical solid and dashed black lines denote the observed and WRF-control driven maximum discharges. The dash-spaced black line represents the ensemble median peak discharge. The light gray shaded area depicts the ensemble spread between quantiles $q_{0.25}$ and $q_{0.75}$ of the members. Note that $Q_{p(T)}$ s are drawn as solid and dashed dark gray lines.

interpreted cautiously. In addition, findings on the probabilistic hydro-meteorological forecasting chain are just illustrative, but enlight the benefits of using an HEPS before such dangerous flash-flood situations.

We expect that further work will allow to account for uncertainties associated with different physical parametrizations of the WRF model (i.e., cloud microphysics, moist convection and boundary-layer schemes) in order to determine the model sensitivity to the atmospheric processes leading to the high precipitation amounts. Further application and evaluation of these methods to a broader climatology might also improve the forecasting and warning schemes presented herein, and will better establish their confidence levels from an operational perspective. However, despite the current limitations, the benefits from hydrometeorological analyses as shown here are of greater significance than its possible weaknesses, given the hazardous consequences and relatively short recurrence periods of these hydrometeorological extremes over the Mediterranean Spain.

Acknowledgments

Two anonymous reviewers are acknowledged for their efforts to improve the quality and contents of this manuscript. Dr. Charles A.

Doswell III is deeply appreciated for his valuable comments and suggestions on this work. The Hydrographic Confederation of the Segura river (CHS) and, in special, Mr. Fernando Toledano Sánchez, head of the management of the observational networks of the CHS, are acknowledged for providing the SAIH rain and flow data. The Spanish Agency of Meteorology (AEMET) is also acknowledged for providing the automatic weather stations precipitation data. This work has been sponsored by CGL2011-24458 (PREDIMED) Spanish project, which is partially supported with FEDER funds.

References

- Addor, N., Jaun, S., Fundel, F., Zappa, M., 2011. An operational hydrological ensemble prediction system for the city of Zurich (Switzerland): skill, case studies and scenarios. *Hydrol. Earth Syst. Sci.* 15, 2327–2347.
- Amengual, A., Romero, R., Gómez, M., Martín, A., Alonso, S., 2007. A hydrometeorological modeling study of a flash flood event over Catalonia, Spain. *J. Hydrometeorol.* 8, 282–303.
- Amengual, A., Romero, R., Alonso, S., 2008. Hydrometeorological ensemble simulations of flood events over a small basin of Majorca Island, Spain. *Q. J. R. Meteorol. Soc.* 134, 1221–1242.
- Amengual, A., Romero, R., Vich, M., Alonso, S., 2009. Inclusion of potential vorticity uncertainties into a hydrometeorological forecasting chain: application to a medium size basin of Mediterranean Spain. *Hydrol. Earth Syst. Sci.* 13, 793–811.

- Bartholmes, J.C., Thielen, J., Ramos, M.H., Gentilini, S., 2009. The European flood alert system EFAS part 2: statistical skill assessment of probabilistic and deterministic operational forecasts. *Hydrol. Earth Syst. Sci.* 13, 141–153.
- Benoit, R., Kouwen, N., Yu, W., Chamberland, S., Pellerin, P., 2003. Hydrometeorological aspects of the real-time ultrafinescale forecast support during the special observing period of the MAP. *Hydrol. Earth Syst. Sci.* 7, 877–889.
- Bhagarva, M., Danard, M., 1994. Application of optimum interpolation to the analysis of precipitation in complex terrain. *J. Appl. Meteorol.* 33, 508–518.
- Borga, M., Boscolo, P., Zanon, F., Sangati, M., 2007. Hydrometeorological analysis of the 29 august 2003 flash flood in the eastern Italian Alps. *J. Hydrometeorol.* 8, 1049–1067.
- Branković, C., Matjajić, B., Ivatek-Sahdan, S., 2008. Downscaling of ECMWF ensemble forecasts for cases of severe weather: ensemble statistics and cluster analysis. *Mon. Weather Rev.* 136, 3323–3342.
- Buizza, R., Palmer, T.N., 1995. The singular-vector structure of the atmospheric general circulation. *J. Atmos. Sci.* 52, 1434–1456.
- Capel, J.M., 1974. Génesis de las inundaciones de Octubre de 1973 en el sureste de la Península Ibérica. *Cuad. Geogr. Univ. Granada* 4, 149–166.
- Capel, J.M., 1989. Convección profunda sobre el Mediterráneo Español. Lluvias torrenciales durante los días 4 al 7 de Septiembre de 1989 en Andalucía oriental, Murcia, Levante, Cataluña y Mallorca. *Paralelo* 13, 51–79.
- Chancibault, K., Anquetin, S., Ducrocq, V., Saulnier, G.-M., 2006. Hydrological evaluation of high-resolution precipitation forecasts of the Gard flash flood event (8–9 September 2002). *Q. J. R. Meteorol. Soc.* 132, 1091–1117.
- Chow, V.T., Maidment, D.R., Mays, L.W., 1988. *Applied hydrology*. Civil Engineering Series. McGraw-Hill International Editions (572 pp.).
- Clark, A.J., Kain, J.S., Stensrud, D.J., Xue, M., Kong, F., Coniglio, M.C., Thomas, K.W., Wang, Y., Brewster, K., Gao, J., Wang, X., Weiss, S.J., Du, J., 2011. Probabilistic precipitation forecast skill as a function of ensemble size and spatial scale in a convection-allowing ensemble. *Mon. Weather Rev.* 139, 1410–1418.
- Cloke, H.L., Pappenberger, F., 2009. Ensemble flood forecasting: a review. *J. Hydrol.* 375, 613–626.
- Cloke, H.L., Pappenberger, F., van Andel, S.J., Schaake, J., Thielen, J., Ramos, M.-H. (Eds.), 2013. Special issue on hydrological ensemble prediction systems (HEPS). *Hydrol. Process.* 27 (1), 1–163.
- Doswell, C.A., Brooks, H.E., Maddox, R.A., 1996. Flash flood forecasting: an ingredients-based methodology. *Weather Forecast.* 11, 560–581.
- Doswell, C.A., Ramis, C., Romero, R., Alonso, S., 1998. A diagnostic study of three heavy precipitation episodes in the Western Mediterranean region. *Weather Forecast.* 13, 102–124.
- Drobinski, P., Font, J., Tintoré, J., Wernli, H., 2014. HyMeX: a 10-year multidisciplinary program on the Mediterranean water cycle. *Bull. Amer. Meteor. Soc.* 95 (7), 1063–1082.
- Du, J., Mullen, S.L., Sanders, F., 1997. Short-range ensemble forecasting of quantitative precipitation. *Mon. Weather Rev.* 125, 2427–2459.
- Ducrocq, V., et al., 2014. HyMeX-SOP1, the field campaign dedicated heavy precipitation and flash flooding in the northwestern Mediterranean. *Bull. Am. Meteorol. Soc.* <http://dx.doi.org/10.1175/BAMS-D-12-00244.1>.
- Ebert, E.E., 2001. Ability of poor man's ensemble to predict the probability and distribution of precipitation. *Mon. Weather Rev.* 129, 2461–2480.
- Epstein, E.S., 1969. Stochastic dynamic prediction. *Tellus* 21, 739–759.
- Ferraris, L., Rudari, R., Siccardi, F., 2002. The uncertainty in the prediction of flash floods in the Northern Mediterranean environment. *J. Hydrometeorol.* 3, 714–727.
- Gil-Olcina, A., 1968. El régimen del río Guadalentín. *Cuad. Geogr.* 5, 163–182.
- Hong, S.-Y., Lim, J.-O.J., 2006. The WRF single-moment 6-class microphysics scheme (WSM6). *J. Korean Meteorol. Soc.* 42 (2), 129–151.
- Houtekamer, P.L., Derome, J., 1995. Methods for ensemble prediction. *Mon. Weather Rev.* 123, 2181–2196.
- INUNMUR, 2007. Plan Especial de Protección Civil ante el riesgo de inundaciones de la Comunidad Autónoma de la Región de Murcia. Dirección General de Protección Civil. Consejería de Desarrollo Sostenible y Ordenación de Territorio, Región de Murcia (418 pp.).
- Janjić, Z.I., 1994. The step-mountain eta coordinate model: further developments of the convection, viscous sublayer and turbulence closure schemes. *Mon. Weather Rev.* 122, 927–945.
- Jasper, K., Kaufmann, P., 2003. Coupled runoff simulations as validation tools for atmospheric models at the regional scale. *Q. J. R. Meteorol. Soc.* 129, 673–692.
- Jolliffe, I.T., Stephenson, D.B., 2003. *Forecast Verification. A Practitioner's Guide in Atmospheric Science*. John Wiley and Sons Ltd., Chichester, West Sussex, England (240 pp.).
- Junker, N.W., Brennan, M.J., Pereira, F., Bodner, M.J., Grumm, R.H., 2009. Assessing the potential for rare precipitation events with standardized anomalies and ensemble guidance at the Hydrometeorological Prediction Center. *Bull. Am. Meteorol. Soc.* 90, 445–453.
- Kain, J.S., 2004. The Kain–Fritsch convective parameterization: an update. *J. Appl. Meteorol.* 43 (1), 170–181.
- Kolios, S., Feidas, H., 2010. Warm season climatology of mesoscale convective systems in the Mediterranean basin using satellite data. *Theor. Appl. Climatol.* 102 (1–2), 29–42.
- Krajewski, W.F., 1987. Cokriging radar-rainfall and rain gauge data. *J. Geophys. Res.* 92 (D8), 9571–9580.
- Leith, C.E., 1974. Theoretical skill of Monte Carlo forecasts. *Mon. Weather Rev.* 102, 409–418.
- Llasat, M.C., Llasat-Botija, M., Prat, M.A., Porcú, F., Price, C., Mugnai, A., Lagouvardos, K., Kotroni, V., Katsanos, D., Michaelides, S., Yair, Y., Savvidou, K., Nicolaides, K., 2010. High-impact floods and flash floods in Mediterranean countries: the FLASH preliminary database. *Adv. Geosci.* 23, 47–55.
- Marsigli, C., Boccanera, F., Moltani, A., Paccagnella, T., 2005. The COSMO-LEPS ensemble system: validation of the methodology and verification. *Nonlinear Process. Geophys.* 12, 527–536.
- Molteni, F., Buizza, R., Palmer, T.N., Petroliagis, T., 1996. The ECMWF ensemble prediction system: methodology and validation. *Q. J. R. Meteorol. Soc.* 122, 73–119.
- Mullen, S.L., Baumhufner, D.P., 1988. Sensitivity to numerical simulations of explosive oceanic cyclogenesis to changes in physical parameterizations. *Mon. Weather Rev.* 116, 2289–2329.
- Nash, J.E., Sutcliffe, J.V., 1970. River flow forecasting through conceptual models. Part I: a discussion of principles. *J. Hydrol.* 10 (3), 282–290.
- Rabuffetti, D., Ravazzani, G., Corbari, C., Mancini, M., 2008. Verification of operational Quantitative Discharge Forecast (QDF) for a regional warning system—the AMPHORE case studies in the upper Po River. *Nat. Hazards Earth Syst. Sci.* 8 (1), 161–173.
- Ranzi, R., Bacchi, B., Grossi, G., 2003. Runoff measurements and hydrological modelling for the estimation of rainfall volumes in an alpine basin. *Q. J. R. Meteorol. Soc.* 129, 653–672.
- Schumann, M.R., Roebber, P.J., 2010. The influence of upper-tropospheric potential vorticity on convective morphology. *Mon. Weather Rev.* 138, 463–474.
- Seo, D.J., 1998. Real-time estimation of rainfall fields using radar rainfall and rain gauge data. *J. Hydrol.* 208, 37–52.
- Siccardi, F., 1996. Rainstorm hazards and related disasters in the western Mediterranean region. *Remote Sens. Rev.* 14, 5–21.
- Toth, Z., Kalnay, E., 1993. Ensemble forecasting at NMC: the generation of perturbations. *Bull. Am. Meteorol. Soc.* 74, 2317–2330.
- US Army Corps of Engineers Hydrologic Engineering Center, 1998. HEC-HMS Hydrologic Modeling System User's Manual. USACE-HEC, Davis, California (188 pp.).
- US Army Corps of Engineers Hydrologic Engineering Center, 2000. Hydrologic modeling system HEC-HMS. Technical Reference Manual. USACE-HEC, Davis, California (157 pp.).
- US Department of Agriculture, 1986. Urban hydrology for small watersheds. Technical Release 55. Nature Resources Conservation Service, US Department of Agriculture, Washington DC, USA.
- Verbunt, M., Walser, A., Gurtz, J., Montani, A., Schär, C., 2007. Probabilistic flood forecasting with a limited-area ensemble prediction system: selected case studies. *J. Hydrometeorol.* 8, 897–909.
- Vincendon, B., Ducrocq, V., Nuissier, O., Vié, B., 2011. Perturbation of convection-permitting NWP forecasts for flash-flood ensemble forecasting. *Nat. Hazards Earth Syst. Sci.* 11, 1529–1544.
- Wilks, D.S., 2006. *Statistical Methods in the Atmospheric Sciences*. Second edition. Elsevier Academic Press Publications, International Geophysics Sciences (627 pp.).
- Zappa, M., Jaun, S., Germann, U., Walser, A., Fundel, F., 2011. Superposition of three sources of uncertainties in operational flood forecasting chains. *Atmos. Res.* 100, 246–262.